Summary

- Subject ID: 17
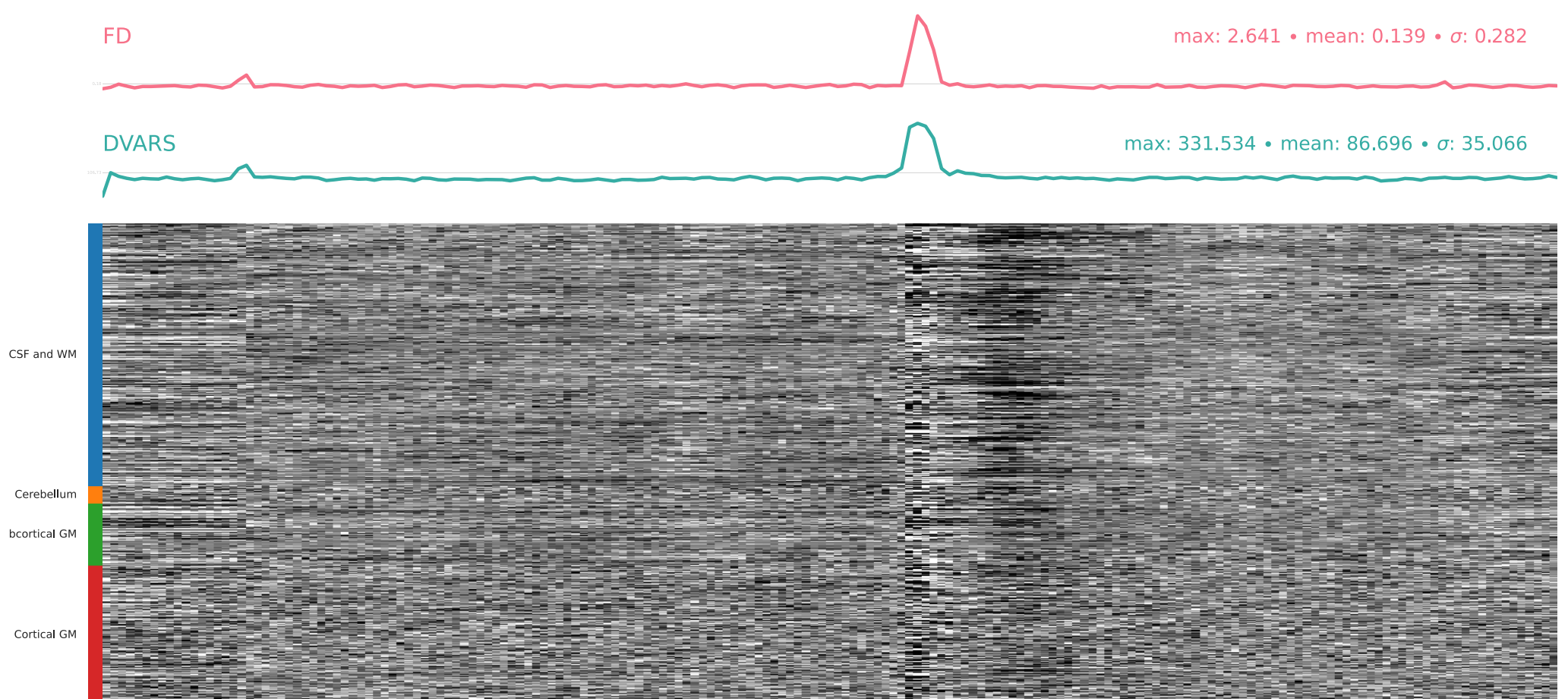- BOLD series: 4

Processing Summary

Reports for: task happy.

Summary

- BOLD volume space: MNI152NLin2009cAsyms
- Repetition Time (TR): 1s
- Mean Framewise Displacement: 0.0944
- Mean Relative RMS Motion: 0.057
- Max Relative RMS Motion: 0.1056
- DVARS Before and After Processing : 80.9232,9.1274
- Correlation between DVARS and FD Before and After Processing : 0.2909, 0.1733
- Number of Volumes Censored : 8
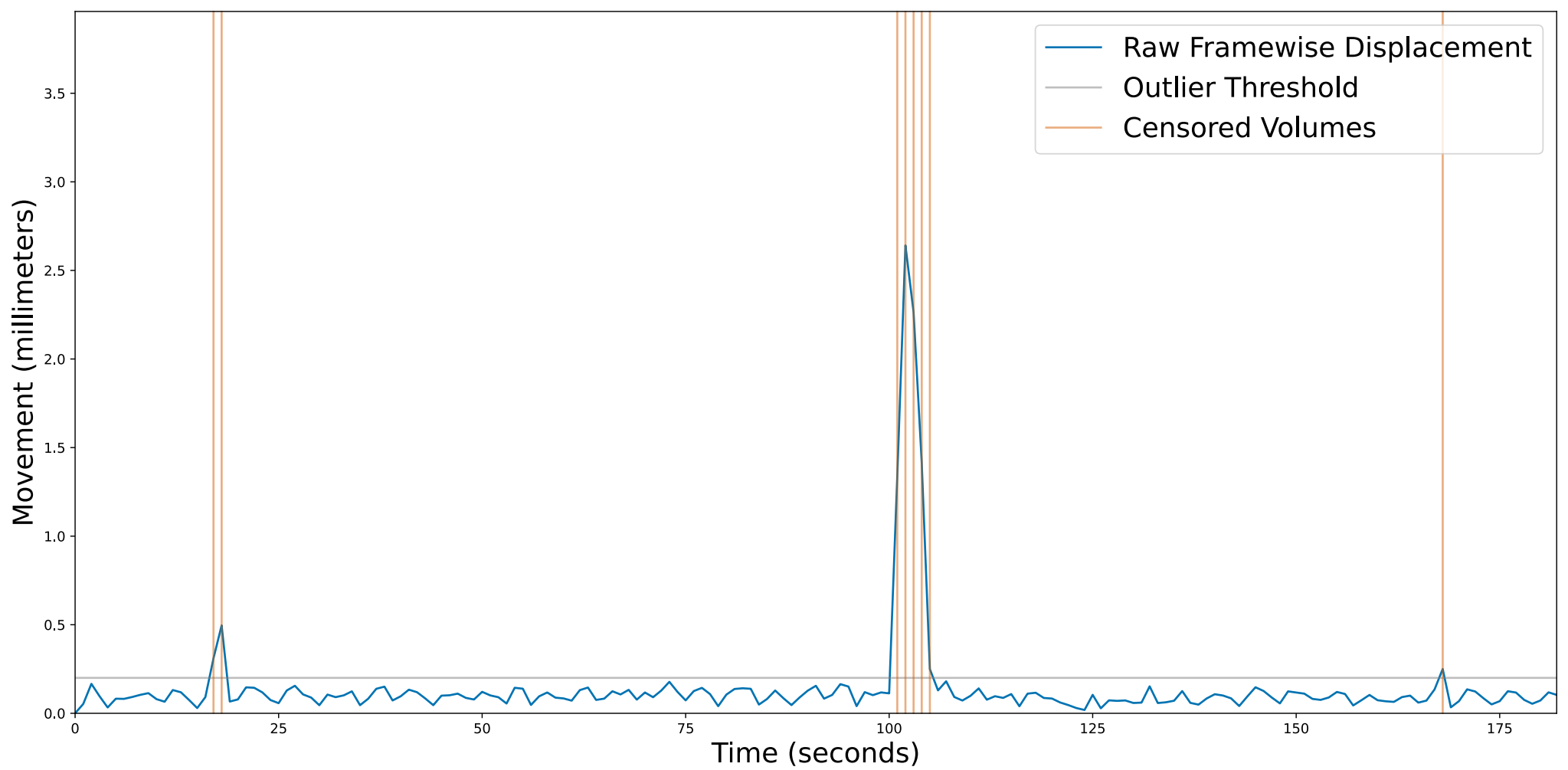
Carpet Plot Before Postprocessing

FD and DVARS are two measures of in-scanner motion. This plot shows standardized FD, DVARS, and then a carpet plot for the time series of each voxel/vertex's time series of activity.

Get figure file: sub-17/figures/sub-17_task-happy_space-MNI152NLin2009cAsym_desc-preprocessing_bold.svg
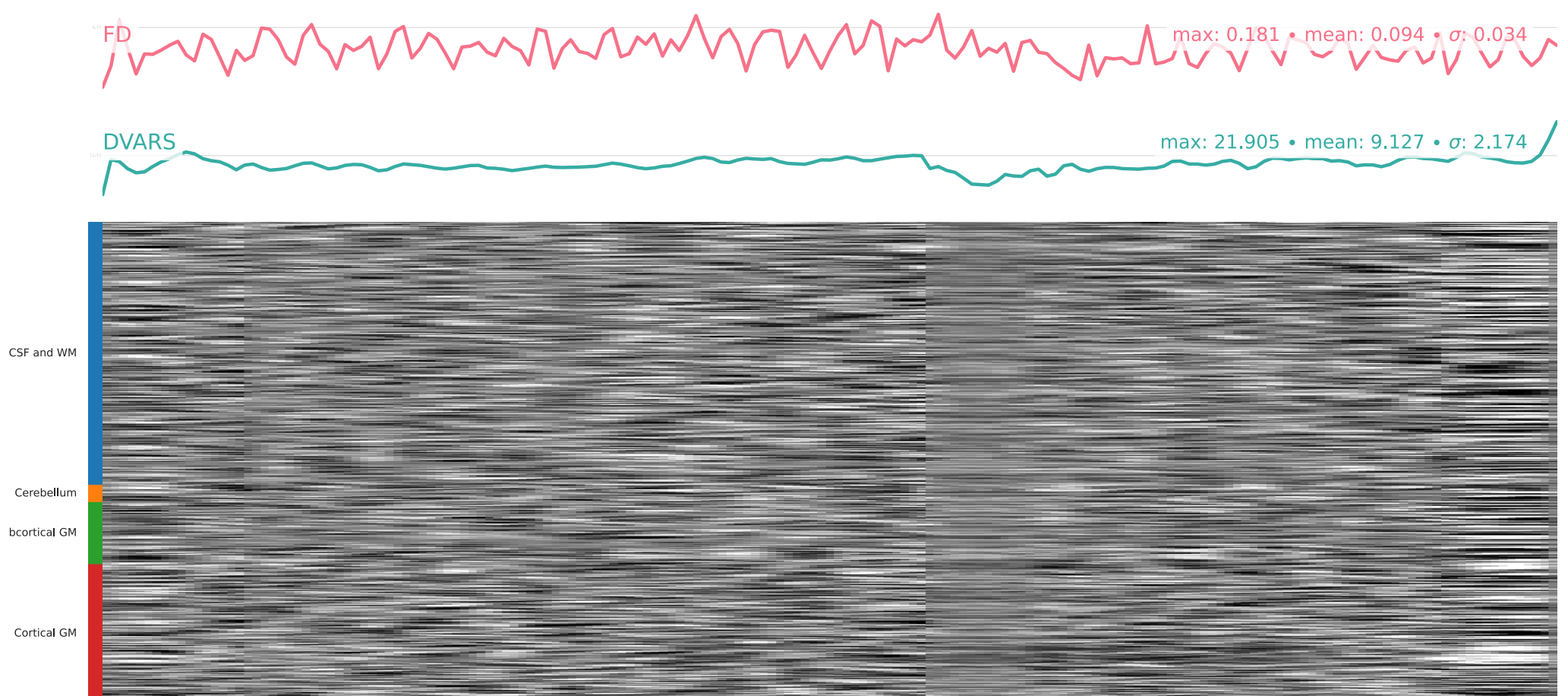
Framewise Displacement and Censored Volumes

Framewise displacement (FD) is used to flag high-motion volumes, which are then censored as part of the denoising procedure. If motion filtering is requested, then the six translation and rotation motion parameters are filtered to remove respiratory effects before FD is calculated and outlier volumes are identified.

Get figure file: sub-17/figures/sub-17_task-happy_space-MNI152NLin2009cAsym_desc-censoring_motion.svg

Carpet Plot After Postprocessing

FD and DVARS are two measures of in-scanner motion. This plot shows standardized FD, DVARS, and then a carpet plot for the time series of each voxel/vertex's time series of activity..

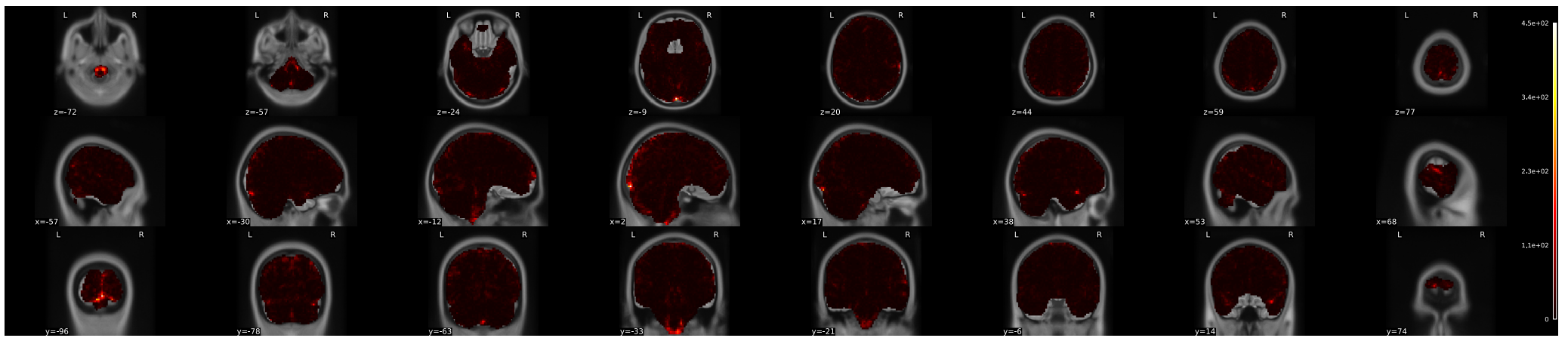Get figure file: sub-17/figures/sub-17_task-happy_space-MNI152NLin2009cAsym_desc-postprocessing_bold.svg

Correlation Heatmaps from Four Atlases

This plot shows heatmaps from ROI-to-ROI correlations from four atlases.

Get figure file: sub-17/figures/sub-17_task-happy_space-MNI152NLin2009cAsym_desc-connectivityplot_bold.svg
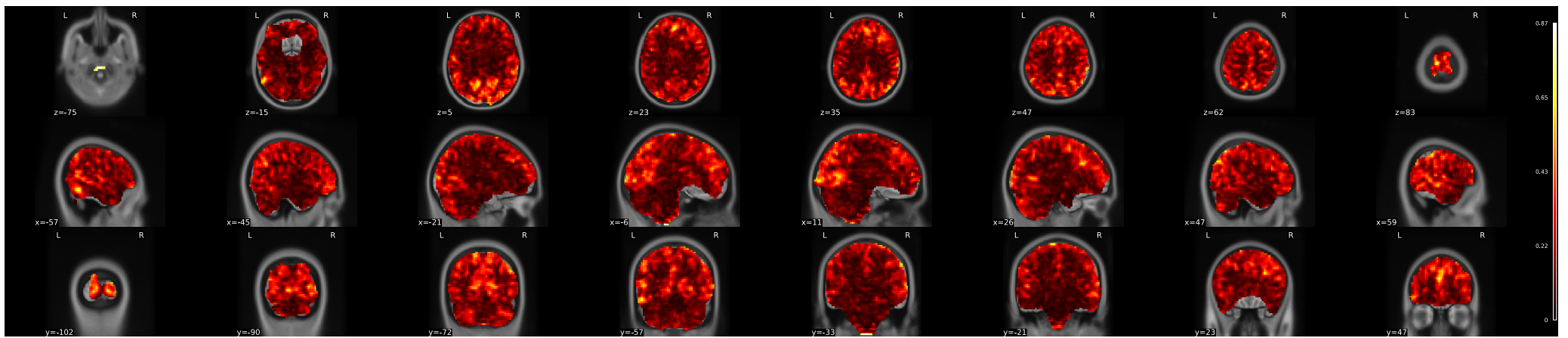
ALFF

ALFF, or amplitude of low frequency fluctuations. Overlaid on T1W image with same entities as the original image.

Get figure file: sub-17/figures/sub-17_task-happy_space-MNI152NLin2009cAsym_desc-alffVolumetricPlot_bold.svg

ReHo

ReHo, or regional homogeneity. Overlaid on T1W image with same entities as the original image.

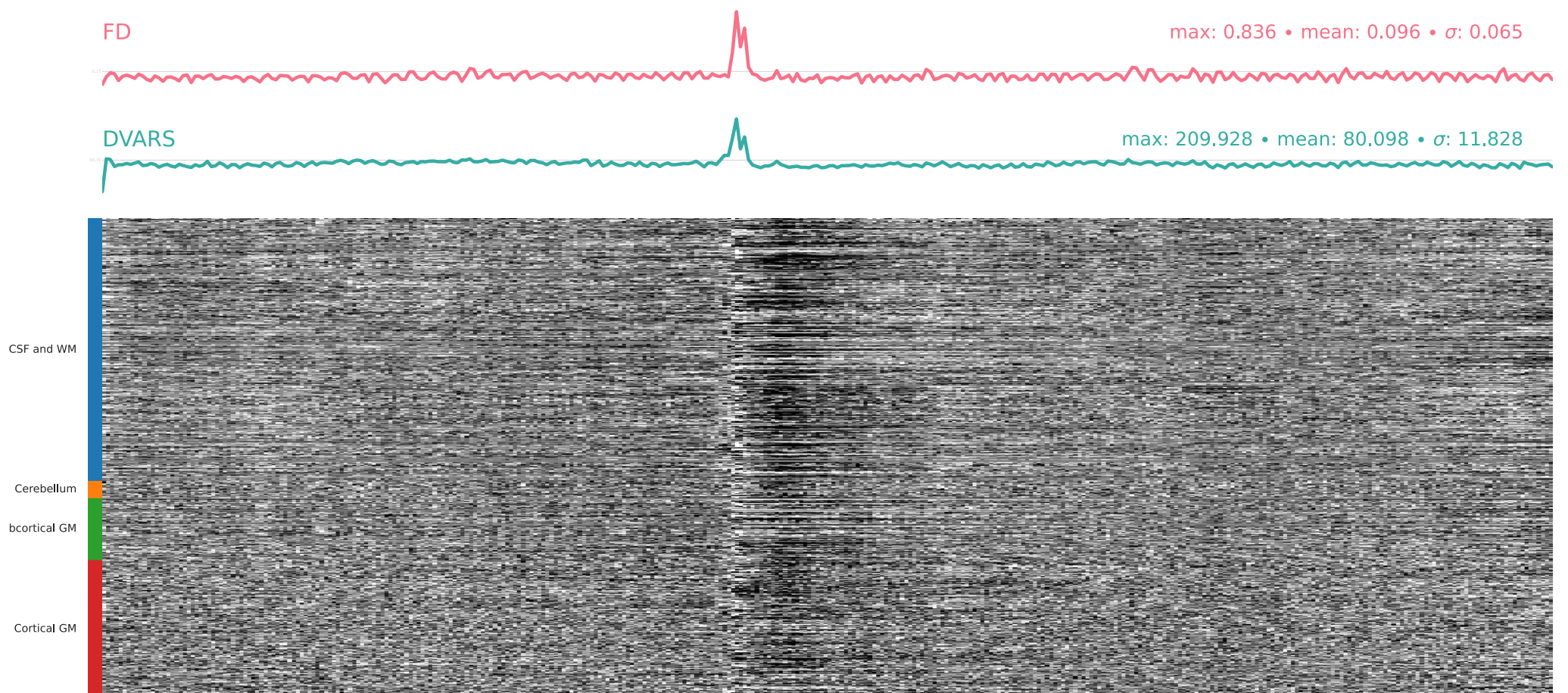Get figure file: sub-17/figures/sub-17_task-happy_space-MNI152NLin2009cAsym_desc-rehoVolumetricPlot_bold.svg

Reports for: task rest.

Summary

- BOLD volume space: MNI152NLin2009cAsyms
- Repetition Time (TR): 1s
- Mean Framewise Displacement: 0.091
- Mean Relative RMS Motion: 0.0573
- Max Relative RMS Motion: 0.1243
- DVARS Before and After Processing : 79.1875,9.8924
- Correlation between DVARS and FD Before and After Processing : 0.337, 0.0024
- Number of Volumes Censored : 4

Carpet Plot Before Postprocessing

FD and DVARS are two measures of in-scanner motion. This plot shows standardized FD, DVARS, and then a carpet plot for the time series of each voxel/vertex's time series of activity.

Get figure file: sub-17/figures/sub-17_task-rest_space-MNI152NLin2009cAsym_desc-preprocessing_bold.svg

Framewise Displacement and Censored Volumes

Framewise displacement (FD) is used to flag high-motion volumes, which are then censored as part of the denoising procedure. If motion filtering is requested, then the six translation and rotation motion parameters are filtered to remove respiratory effects before FD is calculated and outlier volumes are identified.

Get figure file: sub-17/figures/sub-17_task-rest_space-MNI152NLin2009cAsym_desc-censoring_motion.svg

Carpet Plot After Postprocessing

FD and DVARS are two measures of in-scanner motion. This plot shows standardized FD, DVARS, and then a carpet plot for the time series of each voxel/vertex's time series of activity..

Get figure file: sub-17/figures/sub-17_task-rest_space-MNI152NLin2009cAsym_desc-postprocessing_bold.svg

Correlation Heatmaps from Four Atlases

This plot shows heatmaps from ROI-to-ROI correlations from four atlases.

Get figure file: sub-17/figures/sub-17_task-rest_space-MNI152NLin2009cAsym_desc-connectivityplot_bold.svg

ALFF

ALFF, or amplitude of low frequency fluctuations. Overlaid on T1W image with same entities as the original image.

Get figure file: sub-17/figures/sub-17_task-rest_space-MNI152NLin2009cAsym_desc-alffVolumetricPlot_bold.svg

ReHo

ReHo, or regional homogeneity. Overlaid on T1W image with same entities as the original image.

Get figure file: sub-17/figures/sub-17_task-rest_space-MNI152NLin2009cAsym_desc-rehoVolumetricPlot_bold.svg

Reports for: task sadln.

Summary

- BOLD volume space: MNI152NLin2009cAsyms
- Repetition Time (TR): 1s
- Mean Framewise Displacement: 0.0937
- Mean Relative RMS Motion: 0.0532
- Max Relative RMS Motion: 0.1114
- DVARS Before and After Processing : 77.0815,11.2018
- Correlation between DVARS and FD Before and After Processing : 0.3574, -0.0227

- Number of Volumes Censored : 28

Carpet Plot Before Postprocessing

FD and DVARS are two measures of in-scanner motion. This plot shows standardized FD, DVARS, and then a carpet plot for the time series of each voxel/vertex's time series of activity.

Get figure file: sub-17/figures/sub-17_task-sadln_space-MNI152NLin2009cAsym_desc-preprocessing_bold.svg

Framewise Displacement and Censored Volumes

Framewise displacement (FD) is used to flag high-motion volumes, which are then censored as part of the denoising procedure. If motion filtering is requested, then the six translation and rotation motion parameters are filtered to remove respiratory effects before FD is calculated and outlier volumes are identified.

Get figure file: sub-17/figures/sub-17_task-sadln_space-MNI152NLin2009cAsym_desc-censoring_motion.svg

Carpet Plot After Postprocessing

FD and DVARS are two measures of in-scanner motion. This plot shows standardized FD, DVARS, and then a carpet plot for the time series of each voxel/vertex's time series of activity..

Get figure file: sub-17/figures/sub-17_task-sadln_space-MNI152NLin2009cAsym_desc-postprocessing_bold.svg

Correlation Heatmaps from Four Atlases

This plot shows heatmaps from ROI-to-ROI correlations from four atlases.

Get figure file: sub-17/figures/sub-17_task-sadln_space-MNI152NLin2009cAsym_desc-connectivityplot_bold.svg

ALFF

ALFF, or amplitude of low frequency fluctuations. Overlaid on T1W image with same entities as the original image.

Get figure file: sub-17/figures/sub-17_task-sadln_space-MNI152NLin2009cAsym_desc-alffVolumetricPlot_bold.svg

ReHo

ReHo, or regional homogeneity. Overlaid on T1W image with same entities as the original image.

Get figure file: sub-17/figures/sub-17_task-sadln_space-MNI152NLin2009cAsym_desc-rehoVolumetricPlot_bold.svg

Reports for: task sadsh.

Summary

- BOLD volume space: MNI152NLin2009cAsyms
- Repetition Time (TR): 1s
- Mean Framewise Displacement: 0.0902
- Mean Relative RMS Motion: 0.0554
- Max Relative RMS Motion: 0.1163
- DVARS Before and After Processing : 79.4231,9.7294
- Correlation between DVARS and FD Before and After Processing : 0.2224, 0.0253
- Number of Volumes Censored : 18

Carpet Plot Before Postprocessing

FD and DVARS are two measures of in-scanner motion. This plot shows standardized FD, DVARS, and then a carpet plot for the time series of each voxel/vertex's time series of activity.

Get figure file: sub-17/figures/sub-17_task-sadsh_space-MNI152NLin2009cAsym_desc-preprocessing_bold.svg

Framewise Displacement and Censored Volumes

Framewise displacement (FD) is used to flag high-motion volumes, which are then censored as part of the denoising procedure. If motion filtering is requested, then the six translation and rotation motion parameters are filtered to remove respiratory effects before FD is calculated and outlier volumes are identified.

Get figure file: sub-17/figures/sub-17_task-sadsh_space-MNI152NLin2009cAsym_desc-censoring_motion.svg

Carpet Plot After Postprocessing

FD and DVARS are two measures of in-scanner motion. This plot shows standardized FD, DVARS, and then a carpet plot for the time series of each voxel/vertex's time series of activity..

Get figure file: sub-17/figures/sub-17_task-sadsh_space-MNI152NLin2009cAsym_desc-postprocessing_bold.svg

Correlation Heatmaps from Four Atlases

This plot shows heatmaps from ROI-to-ROI correlations from four atlases.

Get figure file: sub-17/figures/sub-17_task-sadsh_space-MNI152NLin2009cAsym_desc-connectivityplot_bold.svg

ALFF

ALFF, or amplitude of low frequency fluctuations. Overlaid on T1W image with same entities as the original image.

Get figure file: sub-17/figures/sub-17_task-sadsh_space-MNI152NLin2009cAsym_desc-alffVolumetricPlot_bold.svg

ReHo

ReHo, or regional homogeneity. Overlaid on T1W image with same entities as the original image.

Get figure file: sub-17/figures/sub-17_task-sadsh_space-MNI152NLin2009cAsym_desc-rehoVolumetricPlot_bold.svg

About

- xcp_d version: 0.3.3rc4+0.gc812fe9.dirty
- xcp_d: `/usr/local/miniconda/bin/xcp_d /fmriprep /out participant -w /work --smoothing 6 --participant_label 15 17`
- xcp_d preprocessed: 2023-03-26 18:16:39 +0000

Methods

We kindly ask to report results preprocessed with this tool using the following boilerplate.

| HTML | Markdown | LaTeX |

Post-processing of fmriprep outputs

The eXtensible Connectivity Pipeline (XCP) (Ciric et al. 2018; Satterthwaite et al. 2013) was used to post-process the outputs of fMRIPrep version 21.0.2 (Esteban et al. 2019, 2020, RRID:SCR_016216). XCP was built with *Nipype* 1.8.5 (Gorgolewski et al. 2011, RRID:SCR_002502). For each of the four BOLD series found per subject (across all tasks and sessions), the following post-processing was performed. First, outlier detection was performed. In order to identify high-motion outlier volumes, framewise displacement was calculated using the formula from Power et al. (2014), with a head radius of 50 mm. Volumes with framewise displacement greater than 0.2 mm were flagged as outliers and excluded from nuisance regression (Power et al. 2014).

Next, the BOLD data and confounds were mean-centered and linearly detrended. In total, 36 nuisance regressors were selected from the preprocessing confounds. These nuisance regressors included six motion parameters, mean global signal, mean white matter signal, mean CSF signal with their temporal derivatives, and the quadratic expansion of six motion parameters, tissues signals and their temporal derivatives (Ciric et al. 2017; Satterthwaite et al. 2013). These nuisance regressors were regressed from the BOLD data using linear regression, as implemented in nilearn 0.9.2 (Abraham et al. 2014). Any volumes censored earlier in the workflow were then interpolated in the residual time series produced by the regression. The interpolated timeseries were then band-pass filtered to retain signals within the 0.009-0.08 Hz frequency band. The processed BOLD was smoothed using Nilearn with a gaussian kernel size of 6.0 mm (FWHM).

Processed functional timeseries were extracted from the residual BOLD signal with *Nilearn's* (version 0.9.2, Abraham et al. 2014) *NiftiLabelsMasker* for the following atlases: the Schaefer 17-network 100, 200, 300, 400, 500, 600, 700, 800, 900, and 1000 parcel atlas (Schaefer et al. 2018), the Glasser atlas (Glasser et al. 2016), the Gordon atlas (Gordon et al. 2016), and the Tian subcortical artlas (Tian et al. 2020). Corresponding pair-wise functional connectivity between all regions was computed for each atlas, which was operationalized as the Pearson's correlation of each parcel's unsmoothed timeseries.

Regional homogeneity (ReHo) was computed with neighborhood voxels using *3dReHo* in AFNI (Cox and Hyd 1997). The amplitude of low-frequency fluctuation (ALFF) (Zou et al. 2008) was computed by transforming the processed BOLD timeseries to the frequency domain. The power spectrum was computed within the 0.009-0.08 Hz frequency band and the mean square root of the power spectrum was calculated at each voxel to yield voxel-wise ALFF measures. The ALFF maps were smoothed with Nilearn using a gaussian kernel size of 6.0 mm (FWHM).

Many internal operations of *XCP* use *TemplateFlow* version 0.8.1 (Ciric et al. 2022), *Nibabel* version 4.0.2 (Brett et al. 2022), *numpy* version 1.18.5 (Harris et al. 2020), and *scipy* version 1.9.3 (Virtanen et al. 2020). For more details, see the *xcp_d* website https://xcp-d.readthedocs.io.

Copyright Waiver

References

Abraham, Alexandre, Fabian Pedregosa, Michael Eickenberg, Philippe Gervais, Andreas Mueller, Jean Kossaifi, Alexandre Gramfort, Bertrand Thirion, and Gael Varoquaux. 2014. "Machine Learning for Neuroimaging with Scikit-Learn." *Frontiers in Neuroinformatics*. https://doi.org/10.3389/fninf.2014.00014.

Brett, Matthew, Christopher J. Markiewicz, Michael Hanke, Marc-Alexandre Côté, Ben Cipollini, Paul McCarthy, Dorota Jarecka, et al. 2022. *Nipy/Nibabel:* (version 4.0.0). Zenodo. https://doi.org/10.5281/zenodo.591597.

Ciric, Rastko, Adon F. G. Rosen, Guray Erus, Matthew Cieslak, Azeez Adebimpe, Philip A. Cook, Danielle S. Bassett, Christos Davatzikos, Daniel H. Wolf, and Theodore D. Satterthwaite. 2018. "Mitigating Head Motion Artifact in Functional Connectivity MRI." *Nature Protocols* 13 (12): 2801–26. https://doi.org/10.1038/s41596-018-0065-y.

Ciric, Rastko, William H Thompson, Romy Lorenz, Mathias Goncalves, Eilidh MacNicol, Christopher J Markiewicz, Yaroslav O Halchenko, et al. 2022. "TemplateFlow: FAIR-Sharing of Multi-Scale, Multi-Species Brain Models." *bioRxiv*. Cold Spring Harbor Laboratory, 2021–02. https://doi.org/10.1101/2021.02.10.430678.

Ciric, Rastko, Daniel H. Wolf, Jonathan D. Power, David R. Roalf, Graham Baum, Kosha Ruparel, Russell T. Shinohara, et al. 2017. "Benchmarking of Participant-Level Confound Regression Strategies for the Control of Motion Artifact in Studies of Functional Connectivity." *NeuroImage* 154 (July): 174–87. https://doi.org/10.1016/j.neuroimage.2017.03.020.

Cox, Robert, and James Hyd. 1997. "Software Tools for Analysis and Visualization of fMRI Data." *NMR in Biomedicine* 10 (4-5): 171–78. https://doi.org/10.1002/(sici)1099-1492(199706/08)10:4/5<171::aid-nbm453>3.0.co;2-l.

Esteban, Oscar, Rastko Ciric, Karolina Finc, Ross W Blair, Christopher J Markiewicz, Craig A Moodie, James D Kent, et al. 2020. "Analysis of Task-Based Functional Mri Data Preprocessed with fMRIPrep." *Nature Protocols* 15 (7). Nature Publishing Group: 2186–2202. https://doi.org/10.1038/s41596-020-0327-3.

Esteban, Oscar, Christopher J Markiewicz, Ross W Blair, Craig A Moodie, A Ilkay Isik, Asier Erramuzpe, James D Kent, et al. 2019. "FMRIPrep: A Robust Preprocessing Pipeline for Functional Mri." *Nature Methods* 16 (1). Nature Publishing Group: 111–16. https://doi.org/10.1038/s41592-018-0235-4.

Glasser, Matthew F., Timothy S. Coalson, Emma C. Robinson, Carl D. Hacker, John Harwell, Essa Yacoub, Kamil Ugurbil, et al. 2016. "A Multi-Modal Parcellation of Human Cerebral Cortex." *Nature* 536 (7615): 171–78. https://doi.org/10.1038/nature18933.

Gordon, Evan M., Timothy O. Laumann, Babatunde Adeyemo, Jeremy F. Huckins, William M. Kelley, and Steven E. Petersen. 2016. "Generation and Evaluation of a Cortical Area Parcellation from Resting-State Correlations." *Cerebral Cortex* 26 (1): 288–303. https://doi.org/10.1093/cercor/bhu239.

Gorgolewski, Krzysztof, Christopher D. Burns, Cindee Madison, Dav Clark, Yaroslav O. Halchenko, Michael L. Waskom, and Satrajit S. Ghosh. 2011. "Nipype: A Flexible, Lightweight and Extensible Neuroimaging Data Processing Framework in Python." *Frontiers in Neuroinformatics* 5. https://doi.org/10.3389/fninf.2011.00013.

Harris, Charles R., Jarrod K. Millman, Stéfan J. van der Walt, Ralf Gommers, Pauli Virtanen, David Cournapeau, Eric Wieser, et al. 2020. "Array Programming with NumPy." *Nature* 585 (7825): 357–62. https://doi.org/10.1038/s41586-020-2649-2.

Power, Jonathan D., Anish Mitra, Timothy O. Laumann, Abraham Z. Snyder, Bradley L. Schlaggar, and Steven E. Petersen. 2014. "Methods to Detect, Characterize, and Remove Motion Artifact in Resting State fMRI." *NeuroImage* 84 (January): 320–41. https://doi.org/10.1016/j.neuroimage.2013.08.048.

Satterthwaite, Theodore D., Mark A. Elliott, Raphael T. Gerraty, Kosha Ruparel, James Loughead, Monica E. Calkins, Simon B. Eickhoff, et al. 2013. "An Improved Framework for Confound Regression and Filtering for Control of Motion Artifact in the Preprocessing of Resting-State Functional Connectivity Data." *NeuroImage* 64 (January): 240–56. https://doi.org/10.1016/j.neuroimage.2012.08.052.

Schaefer, Alexander, Ru Kong, Evan M. Gordon, Timothy O. Laumann, Xi-Nian Zuo, Avram J. Holmes, Simon B. Eickhoff, and B. T. Thomas Yeo. 2018. "Local-Global Parcellation of the Human Cerebral Cortex from Intrinsic Functional Connectivity MRI." *Cerebral Cortex (New York, N.Y.: 1991)* 28 (9): 3095–3114. https://doi.org/10.1093/cercor/bhx179.

Tian, Ye, Daniel S Margulies, Michael Breakspear, and Andrew Zalesky. 2020. "Topographic Organization of the Human Subcortex Unveiled with Functional Connectivity Gradients." *Nature Neuroscience* 23 (11). Nature Publishing Group: 1421–32. https://doi.org/10.1038/s41593-020-00711-6.

Virtanen, Pauli, Ralf Gommers, Travis E. Oliphant, Matt Haberland, Tyler Reddy, David Cournapeau, Evgeni Burovski, et al. 2020. "SciPy 1.0: Fundamental Algorithms for Scientific Computing in Python." *Nature Methods* 17 (3): 261–72. https://doi.org/10.1038/s41592-019-0686-2.

Zou, Qi-Hong, Chao-Zhe Zhu, Yihong Yang, Xi-Nian Zuo, Xiang-Yu Long, Qing-Jiu Cao, Yu-Feng Wang, and Yu-Feng Zang. 2008. "An Improved Approach to Detection of Amplitude of Low-Frequency Fluctuation (ALFF) for Resting-State fMRI: Fractional ALFF." *Journal of Neuroscience Methods* 172 (1): 137–41. https://doi.org/10.1016/j.jneumeth.2008.04.012.

Errors

No errors to report!